



Electrospinning on a plucked string

Xiaoqing Chen¹ , Youchen Zhang^{1,2} , Xuetao He¹ , Haoyi Li^{1,2,*} , Bin Wei¹ , and Weimin Yang^{1,2}

¹College of Mechanical and Electrical Engineering, Beijing University of Chemical Technology, Beijing 100029, China

²State Key Laboratory of Organic–Inorganic Composites, Beijing 100029, China

Received: 22 May 2018

Accepted: 27 August 2018

Published online:

11 September 2018

© Springer Science+Business Media, LLC, part of Springer Nature 2018

ABSTRACT

Preparation of high-quality nanofibers by electrospinning with low applied voltage and industrial scales remains challenging. A novel differential electrospinning technology for nanofiber preparation was proposed, with which multiple jets are generated from the string by plucking. The spinning principles were investigated, and the operation parameters were optimized. Results showed that lower threshold electric field was required for jets generation by plucked string electrospinning compared with the conventional needleless electrospinning. The finest average diameter of nanofibers with a narrow distribution range of 143 ± 16 nm was obtained at an applied voltage of 25 kV, a PVA concentration of 8 wt%, a rotational speed of 150 rpm and a spinning distance of 7 cm. The maximum yield for single string was as high as 2.64 g h^{-1} at a PVA concentration of 12 wt%. It was demonstrated that the proposed technology is feasible for manufacturing of nanofibers with lower voltage and high productivity as the string could be modularly extended.

Introduction

Polymer nanofibers are commonly characterized of minor diameter (1–100 nm) and high aspect ratio (> 1000) [1]. However, it is difficult to achieve uniform and high-quality nanofibers due to the present technical constraints. In recent years, scholars are increasingly focusing on nanofibers for its large specific surface area, high porosity, remarkable scale effect and surface effect. Some novel characteristics were found in light, heat, magnetism and electricity, promising wide applications in medicine [2–4], filtration [5, 6], food processing [7], sensor [8, 9], textile [10], aviation [11] and energy storage [12]. As the demand for nanofiber keeps increasing, work needs

to be conducted on the optimization of production process.

Electrospinning is a process that produces continuous fibers with submicron range of diameter with an external electric field imposed on the polymer melt or solution. It is an efficient and versatile technique for the design of controllable morphology and diameter nanofibers [13, 14]. Compared with single-needle electrospinning, multi-needles electrospinning is more efficient, but lower in quality sourced from the interferential electric field [15]. Besides, the complex structure has also limited its application. Needleless electrospinning is a promising, peculiar method for nanofiber preparation and has been developed in recent years with high-efficiency

Address correspondence to E-mail: lhy@mail.buct.edu.cn

production, nonexistence of needle plugging and convenience of cleaning [16]. The work applying high-voltage static electricity to form self-organized jets from free surface of liquid has been conducted and proved its feasibility. Lucas and Miloh's groups have explained and proved the mechanism of jets self-organization from a free conductive liquid surface [17, 18]. Fundamentally, Li et al. [19, 20] reported an needleless differential electrospinning method using an umbellate nozzles to form jets from liquid free surface, which is suitable and efficient for melt electrospinning. Moreover, new spinning mechanism has been developed. He et al. [21–25] presented bubble electrospinning using bubbles burst phenomenon to initiate jets in a large surface area of solution, where bubbles were generated by blowing compressed air or nitrogen. This technology is a promising candidate for industrialization of nanofibers. In addition, several efforts have been made to improve productivity and quality of electrospinning by modifying the spinneret. Until now, some novel spinnerets have been developed such as rotating disk [26], curved convex slot [27], metal dish [28], rotary cone [29], plate edge [30], multiple ring [31], twisted wire [32] and sprocket wheel disk [33].

So far, those methods are able to improve the throughput of the nanofibers, but request higher applied electric field (generally at least 3 kV cm^{-1}). In addition, the prepared nanofibers have larger diameters and wider diameter distribution compared with single-needle electrospinning, and some of them have electrospun limits for polymer category. High spinning voltage might result in electrostatic breakdown in the volatilization of solvent and safety accidents. Thus, efforts are still needed to reduce spinning voltage and maintain high uniformity of nanofibers in diameter. A needle-disk electrospinning technique was proposed inspired by natural point discharge using multiple needle-disk spinneret, and a narrow diameter distribution of nanofibers was obtained applying a low voltage of 2.5 kV cm^{-1} [34–36]. It was demonstrated that the spinning fluid with an initial velocity favored in overcoming the surface tension and reducing the threshold voltage [37, 38]. However, it is unclear whether it could produce continuous uniform fine nanofibers with both the natural point discharge and initial velocity at low applied voltage.

In this work, we proposed a differential needleless electrospinning method based on a plucked string

with wave mechanics. The movement of the string would generate periodically changed electric field in the spinning area, and the droplets adsorbed on the string would deform and form multiple jets under the combined action of electric field, gravity and inertial force. The effects of solution concentration, applied voltage and rotational speed on nanofibers morphology and diameter distribution were investigated. For a better understanding of the basic principles of this spinning method, string motion and electric field distribution were also analyzed by numerical simulations.

Experimental

Materials

Polyvinyl alcohol (PVA, $M_w = 146000\text{--}186000$; 98–99% hydrolyzed) was purchased from Shanghai Chenqi Chemical Technology Company (China). PVA was chosen as the model polymer to examine the performance of string electrospinning. Sodium dodecyl sulfate (SDS) served as a surfactants additive, obtained from Xilong Chemical Technology Company (China). Prior to solution preparation, PVA powder was swelled in deionized water at $30 \text{ }^\circ\text{C}$ for 30 min. PVA solutions with different concentrations of 8, 9, 10, 11 and 12 wt% were prepared by dissolving PVA powder in deionized water at $90 \text{ }^\circ\text{C}$ with magnetically stirring for 3 h. The soft strings used in this study were obtained from a guitar produced from D'Addario (USA) and made of phosphor bronze with a diameter of 0.38 mm.

String electrospinning apparatus

The string electrospinning apparatus is typically divided into six components: electric motor rotation appliance, string, solution tank, feed pump, high-voltage DC supply and receiver plate (Fig. 1a). The plate receiver was grounded, and high voltage was loaded at one end of the strings with a high-voltage DC supply (Tianjin Dongwen Company, 80 kV). The solution tank was made of polytetrafluoroethylene (PTFE), with a size of $400 \times 80 \times 50 \text{ mm}^3$. The string made of phosphor bronze with a length of 40 cm was installed across the two sides of solution tank. The electric motor rotation appliance containing a rotational shaft and plectrum was connected to the

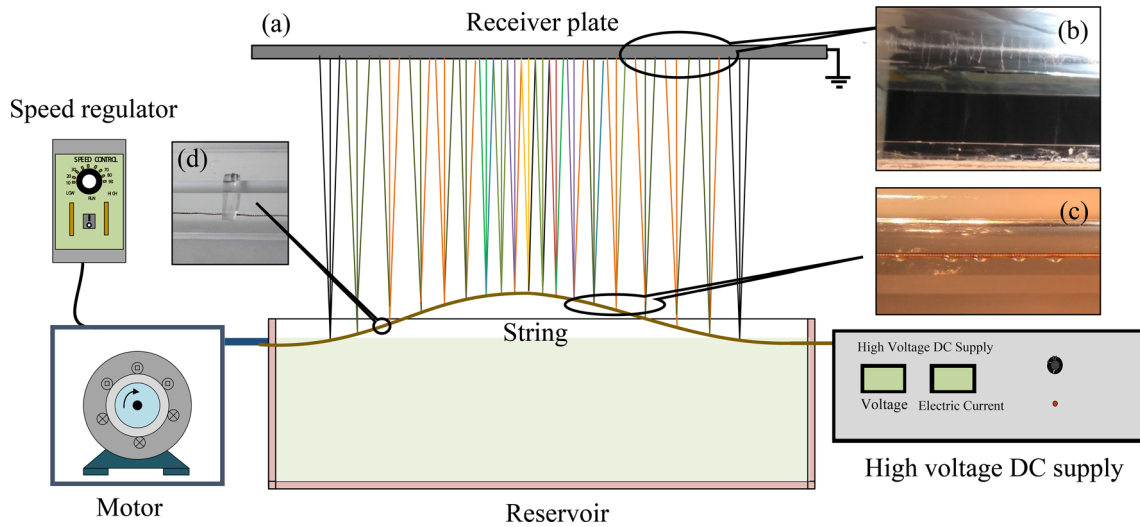


Figure 1 a The schematic diagram of electrospinning device. b The capture of the electrospinning process. c The diagram of solution drops on the string. d The diagram of the string and the plectrum.

solution tank as shown in Fig. 1d. The plate receiver made of aluminum with a size of $400 \times 200 \text{ mm}^2$ was set vertically above the solution-storage tank at an adjustable distance of 0–200 mm. The thickness of the plate receiver was 1 mm.

Characterization

The fiber morphology and diameter were observed by scanning electron microscope (SEM, S4700, Hitachi, Japan). The fiber samples for characterization were prepared by cutting a sample of the aluminum foil target and adhering it to a sample stub with carbon tape and then sputter coating with gold for 2 min (Edwards Sputter Coater S150B) before imaging to minimize charging effect. The average fiber diameter was calculated from the SEM images using the image analysis software (ImagePro + 6.0). Additionally, the electrospinning process was recorded with a digital camera (Canon 600D, Canon, China). The experiments were conducted under the condition of room temperature of $20 \pm 5 \text{ }^\circ\text{C}$ and relative humidity of $20 \pm 5\%$.

Numerical simulation

Simulation of string vibration

String vibration plays an important role in electrospinning with the proposed system, because it would induce the periodical movement and deformation of spinning droplets adsorbed on it. Furthermore, the

electric field in the spinning zone is also closely associated with the vibration of string. Fully understanding string vibration is helpful for the insights into droplet deformation and distribution of electric field. To understand the vibration dynamics of string, numerical simulations were carried out on string vibration. The partial differential equation for the string vibration model applicable to simulate string motion was expressed as [39]

$$u_{tt} = a^2 u_{xx} (0 < x < l, \quad t > 0) \tag{1}$$

The boundary conditions were described as

$$\begin{cases} u(t, 0) = u(t, l) = 0 \\ u(0, x) = \varphi(x) \\ u_t(0, x) = \phi(x) \end{cases} \tag{2}$$

The solution of differential equation can be expressed as

$$\begin{cases} u(t, x) = \sum_{n=1}^{+\infty} \left(C_n \cos \frac{n\pi at}{l} + D_n \sin \frac{n\pi at}{l} \right) \sin \frac{n\pi x}{l} \\ C_n = \frac{2}{l} \int_0^l \varphi(x) \sin \frac{n\pi x}{l} dx \quad (n = 1, 2, 3, \dots) \\ D_n = \frac{2}{n\pi a} \int_0^l \phi(x) \sin \frac{n\pi x}{l} dx \end{cases} \tag{3}$$

where l is the length of the string, x is the position of string on the x -axis, and a is a constant defined as

$$a = \sqrt{u/\rho_v} = \sqrt{F/\rho_v \cdot S} \tag{4}$$

u , ρ_v and S are represented as shear modulus, bulk density and cross-sectional area, respectively. The string vibration equation was solved using MATLAB, and the parameters were set according to Table 1.

Simulation of electric fields

The distribution and size of electric field are the most important factor of spinning quality and productivity. The analysis of electric field simulation is helpful for the understanding of the electrospinning process. Electric field was calculated with the finite element method (FEM) and ANSYS 14.5. The computing model was based on the equation $E = -\nabla V$ (where E is strength of electric field and V is electric potential). The electrical conductivity of air was set to 0.0 S m^{-1} . An electric potential of 20 kV was set on the string located in the solution container, and the receiver plate was set as 0.0 kV. Two-dimensional mesh was built in the simulating zone with a boundary dimension of $50 \times 30 \text{ cm}^2$. The element size was set to 10 mm. The mesh in spinning zone with a length of 40 cm and width of 7 cm was set with the element size for maximization of 20 mm and 5.88 mm. Other parameters used default settings.

Results and discussion

Performance

This needleless electrospinning apparatus based on a plucked string provides a novel method that the spinning jet ejected along the metal string. The electric field varies with the cyclical motion of string. The change made the jet more easily ejected from the droplet dipped on the string, as shown in Fig. 1. The string vibrates to the highest position with the maximum of elastic potential and the minimum of kinetic energy, after which the string begins to move downward. The droplets on the string continuously

move upward to the spinning area and strip due to the inertial dragging force. The floating droplets are subsequently stretched by the electric field to form spinning jets. The polymer solution jets undergo upward stresses from both the electric field and gravity, which make them become thinner. In addition, the device is easier and safer to be operated and requires a relatively lower voltage for initiating jets compared with other needleless electrospinning techniques. Moreover, almost all the nanofibers produced from the string spinneret have smaller diameter than the conventional method electrospun PVA nanofibers.

Effects of processing parameters on PVA nanofibers

Concentration of PVA polymer solution

PVA was selected for string electrospinning tests because it is commonly used in solution electrospinning. It has a relatively narrow concentration range for electrospinning [40]. In order to investigate the effect of PVA concentration on fiber diameter and morphology, PVA solutions with different concentrations of 8–12 wt% were prepared, and the distance between the string and the receiver plate was set to 7 cm, with a constant voltage of 25 kV, a rotational speed of 90 rpm and a single plectrum. Figure 2 presents the SEM images of nanofibers prepared from different PVA solution concentrations. It is found that as the solution concentration increased from 8 to 12 wt%, the average fiber diameter increased from 173 ± 15 to 395 ± 156 nm, respectively, as shown in Fig. 3. It can be seen that fiber diameter and its width of distribution increased gradually with solution concentration. The phenomenon mainly resulted from that the increase in PVA concentration would give rise to stronger cohesive forces between the PVA chains and increased viscosity in the solution, which consequently enhanced the surface tension of solution. It increased the difficulty in the formation and stretching of solution jets.

As shown in Fig. 3, the effect of polymer concentration on the productivity of PVA nanofibers was obvious. With the increase in PVA concentration from 8 to 12 wt%, the nanofiber productivity increased from 1.12 to 2.64 g h^{-1} . This increase in

Table 1 String motion parameters

Parameters	Values
F (string tension)	38.7 N
ρ_v (bulk density)	7.79 g cm^{-3}
S (cross-sectional area)	$4.536 \times 10^3 \text{ cm}^2$
l (string length)	40 cm

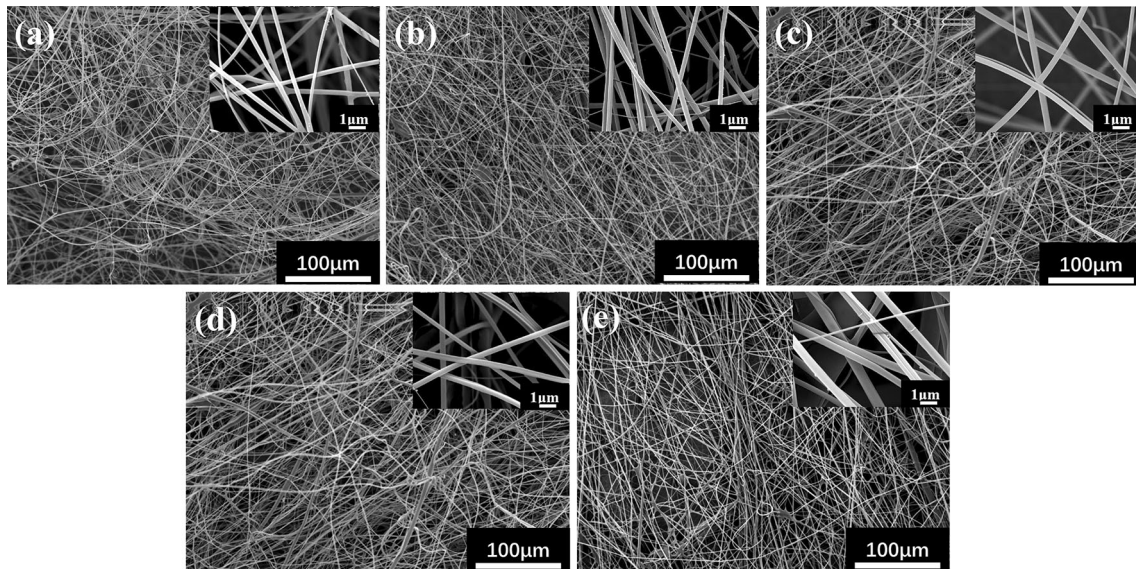


Figure 2 The SEM images of PVA electrospun nanofibers with different solution concentrations. **a** 8 wt%, **b** 9 wt%, **c** 10 wt%, **d** 11 wt%, **e** 12 wt% (spinning distance = 7 cm, applied voltage = 25 kV, rotational speed = 90 rpm, plectrum = 2).

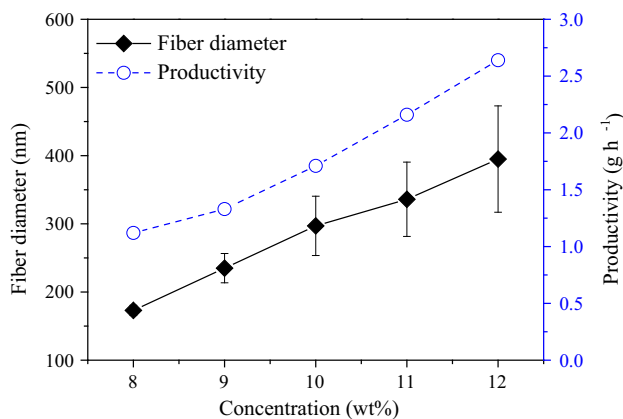


Figure 3 Effect of polymer concentration on average fiber diameter and productivity of nanofibers.

PVA nanofiber productivity was due to the increase in PVA content in higher concentration solutions.

Applied voltage

For the string spinneret, no fiber was generated from the string when the applied voltage was lowered than 12 kV when the solution concentration was 10 wt% and the spinning distance was set to 7 cm. While the applied voltage was above such a critical point, about 14 kV, jets and fibers started to appear from the droplets hanging on the string. Increasing the voltage to 15 kV led to more fibers generation from the string. The strength of the electric field varied over a wide

range. Figure 4 shows the effect of applied voltage on the average diameter of the PVA nanofibers. The applied voltages were set to 15–30 kV with a fixed spinning distance of 7 cm, a constant value of PVA solution concentration of 10 wt%, a rotational speed of 90 rpm and a single plectrum. When the applied voltage was set to a higher level, the surface charge density of solution jets increased and the electrostatic repulsion was enforced. At the same time, with the increase in electric field strength, the tensile stress and strain rate of the nanofibers were fortified, which facilitated the refining of nanofibers and promoted the elongation of jet, hence reducing the diameter and its standard deviation of fibers. The productivity of PVA nanofibers produced at different applied voltages is shown in Fig. 5. It can be found that the productivity increases with applied voltage. The highest productivity reached 2.56 g h⁻¹, 25 times more than conventional single-needle electrospinning (0.1 g h⁻¹) [41].

Rotational speed and plectrum number

The speed of plucking the strings and plectrum number was also considered as significant factors of the diameter and productivity of the nanofibers. In this experiment, the PVA solutions have a concentration range of 8–12 wt%. The rotational speed of the motor was set to 60, 90 and 120 rpm, and the spinning distance was fixed at 7 cm to study the effect of

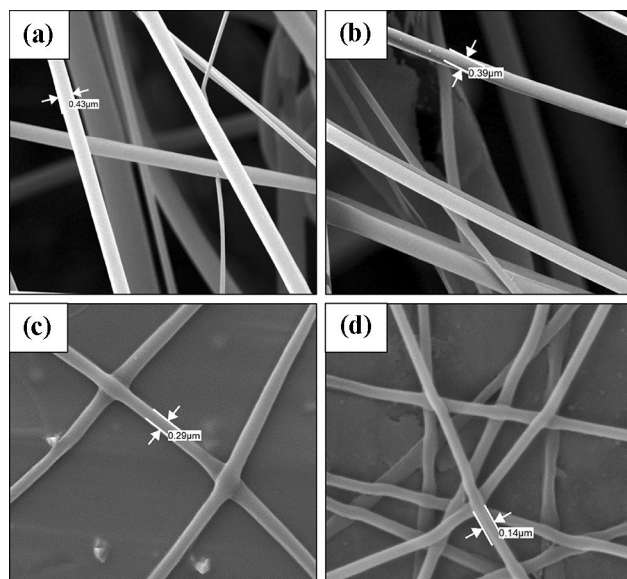


Figure 4 The SEM images of PVA electrospun nanofibers with different applied voltages. **a** 15, **b** 20, **c** 25, **d** 30 kV (spinning distance = 7 cm, PVA solution concentration = 10 wt%, rotational speed = 90 rpm, plectrum = 2).

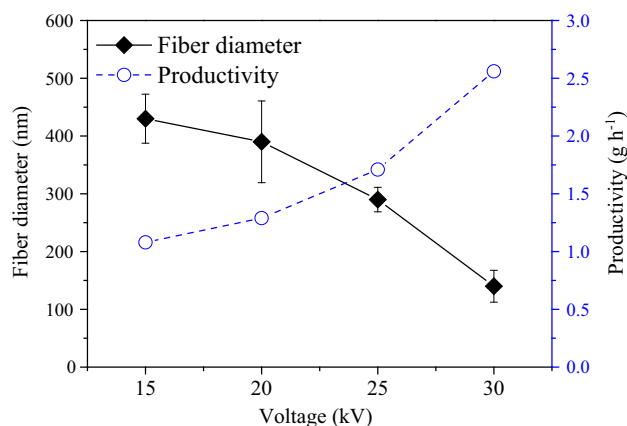


Figure 5 Effect of different applied voltages on average fiber diameter and productivity of nanofibers.

rotational speed. The average fiber diameter showed a slight continuous decrease as the string plucking frequency was increased by raising rotational speed as illustrated in Fig. 6. The average diameters of the electrospun nanofibers decreased by 7.77% when the rotational speed increased from 60 to 90 rpm. It was decreased by 10.65% when the speed increased from 90 to 120 rpm. The finest average diameter of nanofibers with a narrow distribution of 143 ± 16 nm was obtained at an applied voltage of 25 kV, a PVA concentration of 8 wt% and rotational speed of 150 rpm. The productivity was as high as 1.21 g h^{-1} , being 12

times more than single-needle electrospinning. When increasing the rotational speed, the productivity was slightly increased. This means that increasing the vibration frequency of string can slightly enhance the productivity of nanofibers.

The plectrum number was set to one and two to investigate its effect on nanofiber diameter and productivity. All plectrums were set at the position to divide the string length into equal parts. The results revealed that the diameters of PVA nanofiber were 297 ± 87 and 230 ± 43 nm for one and two plectrums, respectively. The corresponding productivities were 1.71 and 2.13 g h^{-1} , respectively. It was

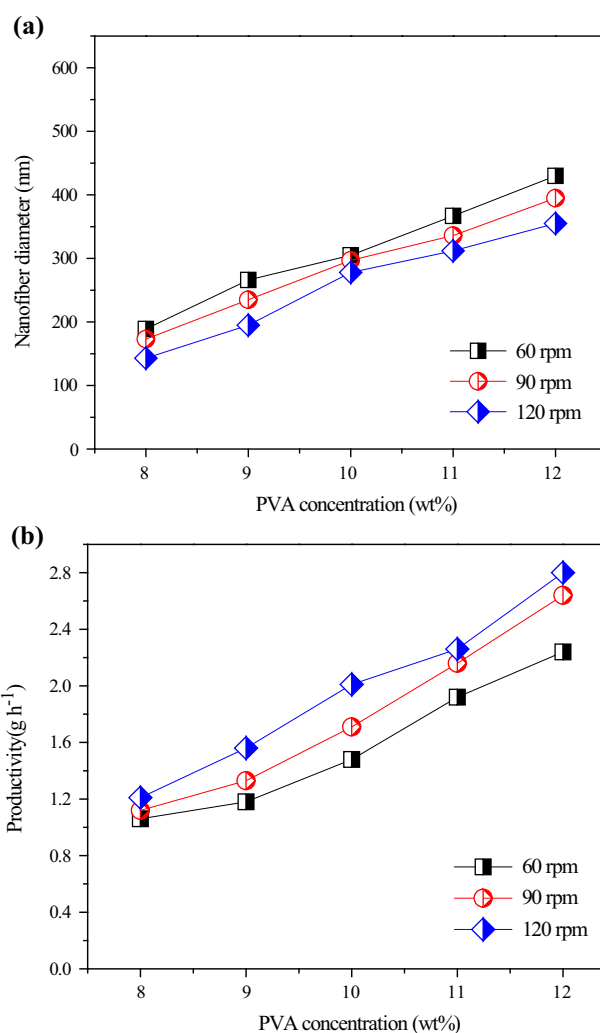


Figure 6 a Diameter of PVA electrospun nanofibers when rotational speeds were 60, 90 and 120 rpm. **b** Productivity of PVA electrospun nanofibers when rotational speeds were 60, 90 and 120 rpm (PVA solution concentrations were ranging from 8 to 12 wt%, spinning distance = 7 cm and applied voltage = 25 kV, plectrum number = 2).

obvious that the plectrum number also has a significant effect on the PVA nanofiber diameter and productivity.

The obtained nanofibers have a narrow diameter distribution for all rotational speeds. Because the size of droplets dipped along the string was uniform, each of them was like the spinneret in traditional single-needle electrospinning. In conclusion, the produced PVA nanofiber has advantages in diameter and productivity when compared with single-needle electrospinning. The device was further simplified. The optimum rotation speed for the considered cases is about 90 rpm, with the balance in energy consumption and device cost.

Numerical simulation analysis

String vibration and electric field analysis

The vibration of string will influence the droplet motion state and electric field distribution in the spinning zone. The situations with different numbers of plectrum were simulated, and the discrepancy between one and two plectrums was apparent (Fig. 7). The string vibrated to the highest position with the maximum of elastic potential energy and the minimum of kinetic energy, after which the string began to move downward. The droplets on the string continuously moved upward to the spinning area and stripped due to inertial force. The floating droplets were subsequently stretched by the electric field forming spinning jets. The wave peak was obtained at the middle of the string with the peak value of 6.5 mm for two plectrums and 6.1 mm for one plectrum. The higher peak was found in the condition of two plectrums contributing to the greater stretched length which endow the string greater elastic potential energy and it converted into more kinetic energy. Furthermore, the string vibrating height up to 5 mm for two plectrums was wider than that of one plectrum which favored to initiate the spinning jet. Therefore, two plectrums were more conducive to spinning for this device.

The distribution and size of electric field directly affect fiber quality and productivity.

The analysis of electric field simulation is helpful to explain the low applied voltage and finer nanofibers of the device [42]. The string vibration influenced the distribution of electric field in spinning area directly

(Fig. 8). Initially, the electric field strength in the spinning zone was appropriately 2.7 kV cm^{-1} , and the maximum electric field intensity reached 4.08 kV cm^{-1} , both of which were located at the ends of the string. While the string vibrated to the highest position, the electric field in most spinning area increased to 3.00 kV cm^{-1} , and the maximum field strength increased to 4.12 kV cm^{-1} . The results showed that electric field distribution varied significantly at different vibration positions. The strengthening of electric field was beneficial for the formation of spinning jets. The vector distributions of the electric field showed that the electric field directed upward fundamentally (Fig. 8c, d). The uniformity of direction ensured the homogeneity of the nanofibers and the deposition on the receiving plate in good order.

Theoretical analysis

It is widely accepted that needleless electrospinning of polymer nanofibers first undergoes wave crest formed at a free liquid surface when gradually increasing applied voltage. Theoretically, Lukas et al. [17] explained that needleless electrospinning polymeric jets could be self-organized from a free conductive liquid surface when the electric field intensity strength exceeds a certain critical value. Moreover, Miloh et al. [18] revealed that on a spherical surface with a uniform liquid layer, polymer jets could be ejected when the external applied electric field strength surpasses a critical value. For conventional needleless electrospinning techniques, multiple jets from the waves crest in a large free liquid surface induced by a critical electric field value are unstable in controlling the number of the jets. So it could cause poor quality of prepared nanofibers.

As for string differential electrospinning, a uniform thin solution layer was repetitively adsorbed on the string surface during the vibration of string. Then, multiple jets were initiated from the free surface of string by electric force when it bounced over the liquid level. The string in the process of movement could induce multiple jets and give the jets an initial kinetic energy. It also changed the electric field strength in the spinning zone simultaneously. It was proved that spinning solution with initial velocity was more inclined to overcome the liquid surface tension to eject a liquid jet [29, 38]. Similarly, it is believed that the initial kinetic energy of multiple jets

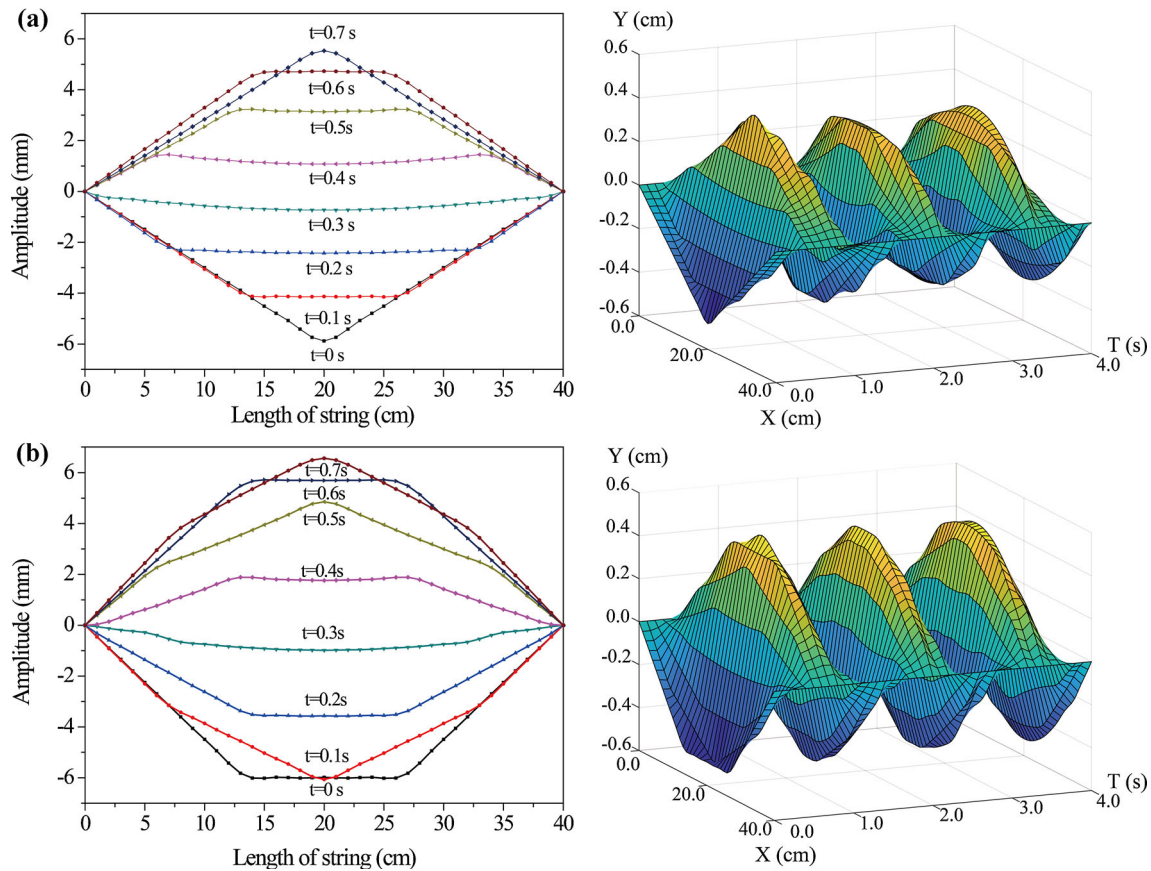


Figure 7 **a** The track of the strings when a pluck is made. **b** The track of the strings when two plucks were set.

helped to stretch and refine the nanofiber sufficiently, leading to a relatively low jet-initiation electric field strength. Rapid change of electric field strength was conducive to the jets initiation. Furthermore, judging from the results, adjusting the speed of the pluck had only slight effect on the movement speed of the string, hence little difference in diameter and morphology of nanofiber. The reason is that the pluck in a suitable speed range could provide enough initial kinetic energy to the string. If the dragging force of the string is overlarge, the initial velocity of the droplets dipped on the string would flung out.

Conclusion

The string had been proved to be an efficient spinneret that can electrospun nanofibers from polymer solution. The generated periodical motion of the string forced by plucking enabled it to start electrospinning at a relatively low applied voltage (15 kV), in which the electric field strength was at about

2.14 kV cm^{-1} . By changing the process parameters, the experimental results revealed that PVA solution concentration and applied voltage had a great effect on the diameter of electrospun nanofibers. The rotor speed has very weak influences on the diameter and productivity. The finest average diameter of nanofibers with a narrow distribution range of $143 \pm 16 \text{ nm}$ was obtained with a voltage of 25 kV, PVA solution concentration of 8 wt%, the rotational speed of 150 rpm and single pluck. Besides, with the same condition, the highest productivity from one string reached 2.64 g h^{-1} , which is 26 times higher than conventional single-needle electrospinning approach. This technique provides a feasible technology for nanofibers manufactured with low applied voltage and high productivity since the string can be modularly extended. Furthermore, an in-depth study of string electrospinning mechanism is necessary and the effect of string type, string diameter, string surface roughness, etc., on spinning process will be investigated in the future.

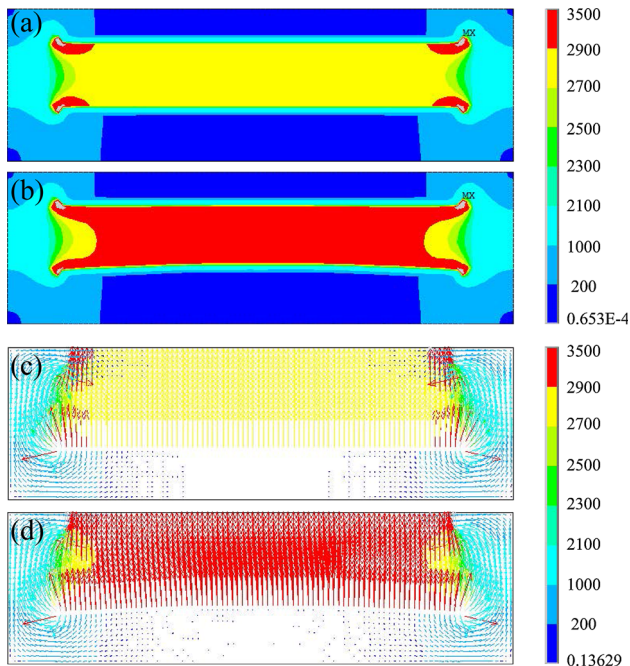


Figure 8 **a** Diagram of electric field strength when the amplitude is 0. **b** Diagram of electric field strength between string and receiver when the amplitude is 6 mm. **c** The vector distribution of the electric field when the amplitude is 0. **d** The vector distribution of the electric field when the amplitude is 6 mm.

Acknowledgements

This work was supported by the National Key Research and Development Program (Grant No. 2016YFB0302002) and National Science Foundation of China (Grant No. 51603009). The reviewers' valuable comments are appreciated and Dr Yiqiang Fan was thanked for the grammar modifications of manuscript. We thank Dr Lisheng Cheng for the major revision improvement and Dr Jiahao Liang for the figures revision and manuscript improvement.

Compliance with ethical standards

Conflict of interest The authors declare that they have no conflict of interest.

References

- [1] Macdiarmid AG, WEJ Jr, Norris ID, Gao J, ATJ Jr, Pinto NJ, Hone J, Han B, Ko FK, Okuzaki H, Llaguno M (2001) Electrostatically-generated nanofibers of electronic polymers. *Synth Met* 119:27–30
- [2] Ramakrishna S, Jose R, Archana PS, Nair AS, Balamurugan R, Venugopal J, Venugopal J, Teo WE (2010) Science and engineering of electrospun nanofibers for advances in clean energy, water filtration, and regenerative medicine. *J Mater Sci* 45:6283–6312. <https://doi.org/10.1007/s10853-010-4509-1>
- [3] Nikmaram N, Roohinejad S, Hashemi S, Koubaa M, Barba FJ, Abbaspourrad A, Greiner R (2017) Emulsion-based systems for fabrication of electrospun nanofibers: food, pharmaceutical and biomedical applications. *RSC Adv* 7:28951–28964
- [4] Xie J, MacEwan MR, Schwartz AG, Xia Y (2010) Electrospun nanofibers for neural tissue engineering. *Nanoscale* 2:35–44
- [5] Sundarajan S, Tan KL, Lim SH, Ramakrishna S (2014) Electrospun nanofibers for air filtration applications. *Proc Eng* 75:159–163
- [6] Kaur S, Rana D, Matsuura T, Sundarajan S, Ramakrishna S (2012) Preparation and characterization of surface modified electrospun membranes for higher filtration flux. *J Membr Sci* 390:235–242
- [7] Mendes AC, Stephansen K, Chronakis IS (2017) Electrospinning of food proteins and polysaccharides. *Food Hydrocoll* 68:53–68
- [8] Tang W, Wang J (2015) Methanol sensing micro-gas sensors of SnO₂-ZnO nanofibers on Si/SiO₂/Ti/Pt substrate via stepwise-heating electrospinning. *J Mater Sci* 50:4209–4220. <https://doi.org/10.1007/s10853-015-8972-6>
- [9] Yao PJ, Wang J, Qiao Q, Du HY (2015) Direct fabrication of La_{0.7}Sr_{0.3}FeO₃ nanofibers with tunable hollow structures by electrospinning and their gas sensing properties. *J Mater Sci* 50:1338–1349. <https://doi.org/10.1007/s10853-014-8694-1>
- [10] Mirjalili M, Zohoori S (2016) Review for application of electrospinning and electrospun nanofibers technology in textile industry. *J Nanostruct Chem* 6:207–213
- [11] Fang W, Yang S, Wang XL, Yuan TQ, Sun RC (2017) Manufacture and application of lignin-based carbon fibers (LCFs) and lignin-based carbon nanofibers (LCNFs). *Green Chem* 19:1794–1827
- [12] Xu H, Hu X, Sun Y, Luo W, Chen C, Liu Y, Huang Y (2014) Highly porous Li₄Ti₅O₁₂/C nanofibers for ultrafast electrochemical energy storage. *Nano Energy* 10:163–171
- [13] Li L, Peng S, Lee JKY, Ji D, Srinivasan M, Ramakrishna S (2017) Electrospun hollow nanofibers for advanced secondary batteries. *Nano Energy* 39:111–139
- [14] He J, Qin T, Liu Y, Li X, Li D, Jin Z (2014) Electrospinning of nanofibrous scaffolds with continuous structure and material gradients. *Mater Lett* 137:393–397
- [15] Nayak R, Padhye R, Kyratzis IL, Truong YB, Arnold L (2012) Recent advances in nanofibre fabrication techniques. *Text Res J* 82:129–147

- [16] Yu M, Dong RH, Yan X, Yu GF, You MH, Ning X, Long YZ (2017) Recent advances in needleless electrospinning of ultrathin fibers: from academia to industrial production. *Macromol Mater Eng* 302:1700002
- [17] Lukas D, Sarkar A, Pokorny P (2008) Self-organization of jets in electrospinning from free liquid surface: a generalized approach. *J Appl Phys* 103:084309
- [18] Miloh T, Spivak B, Yarin AL (2009) Needleless electrospinning: electrically driven instability and multiple jetting from the free surface of a spherical liquid layer. *J Appl Phys* 106:114910
- [19] Li H, Chen H, Zhong X, Wu W, Ding Y, Yang W (2014) Interjet distance in needleless melt differential electrospinning with umbellate nozzles. *J Appl Polym Sci*. <https://doi.org/10.1002/app.40515>
- [20] Li H, Wu W, Bubakir MM, Chen H, Zhong X, Liu Z, Ding Y, Yang W (2014) Polypropylene fibers fabricated via a needleless melt-electrospinning device for marine oil-spill cleanup. *J Appl Polym Sci*. <https://doi.org/10.1002/app.40080>
- [21] Liu Y, He JH, Yu JY (2008) Bubble-electrospinning: a novel method for making nanofibers. *J Phys Conf Ser* 96:012001
- [22] Liu Y, He JH, Xu L, Yu JY (2008) The principle of bubble electrospinning and its experimental verification. *J Polym Eng* 28:55–66
- [23] Yang R, He J, Xu L, Yu J (2009) Bubble-electrospinning for fabricating nanofibers. *Polymer* 50:5846–5850
- [24] He JH, Liu Y (2012) Control of bubble size and bubble number in bubble electrospinning. *Comput Math Appl* 64:1033–1035
- [25] He JH, Kong HY, Yang RR, Hao D (2012) Review on fiber morphology obtained by bubble electrospinning and blown bubble spinning. *Therm Sci* 16:1263–1279
- [26] Niu H, Lin T, Wang X (2009) Needleless electrospinning. I. A comparison of cylinder and disk nozzles. *J Appl Polym Sci* 114:3524–3530
- [27] Yan G, Niu H, Shao H, Zhao X, Zhou H, Lin T (2017) Curved convex slot: an effective needleless electrospinning spinneret. *J Mater Sci* 52:11749–11758. <https://doi.org/10.1007/s10853-017-1315-z>
- [28] Wei L, Yu H, Jia L, Qin X (2018) High-throughput nanofiber produced by needleless electrospinning using a metal dish as the spinneret. *Text Res J* 88:80–88
- [29] Lu B, Wang Y, Liu Y, Duan H, Zhou J, Zhang Z, Wang Y, Li X, Wang W, Lan W, Xie E (2010) Superhigh-throughput needleless electrospinning using a rotary cone as spinneret. *Small* 6:1612–1616
- [30] Thoppey NM, Bochinski JR, Clarke LI, Gorga RE (2010) Unconfined fluid electrospun into high quality nanofibers from a plate edge. *Polymer* 51:4928–4936
- [31] Wang X, Lin T, Wang X (2014) Scaling up the production rate of nanofibers by needleless electrospinning from multiple ring. *Fibers Polym* 15:961–965
- [32] Holopainen J, Penttinen T, Santala E, Ritala M (2014) Needleless electrospinning with twisted wire spinneret. *Nanotechnology* 26:025301
- [33] Ali U, Niu H, Aslam S, Jabbar A, Rajput AW, Lin T (2017) Needleless electrospinning using sprocket wheel disk spinneret. *J Mater Sci* 52:1–11. <https://doi.org/10.1007/s10853-017-0989-6>
- [34] Liu Z, Zhao J, Liu P, He J (2016) Tunable surface morphology of electrospun PMMA fiber using binary solvent. *Appl Surf Sci* 364:516–521
- [35] Liu Z, Chen R, He J (2016) Active generation of multiple jets for producing nanofibres with high quality and high throughput. *Mater Des* 94:496–501
- [36] Liu Z, Ang KKJ, He J (2016) Needle-disk electrospinning inspired by natural point discharge. *J Mater Sci* 52:1–8. <https://doi.org/10.1007/s10853-016-0472-9>
- [37] Hsiao HY, Huang CM, Liu YY, Kuo YC, Chen H (2012) Effect of air blowing on the morphology and nanofiber properties of blowing-assisted electrospun polycarbonates. *J Appl Polym Sci* 124:4904–4914
- [38] Zhang X, Lu Y (2014) Centrifugal spinning: an alternative approach to fabricate nanofibers at high speed and low cost. *Polym Rev* 54:677–701
- [39] Weinberger HF (2012) *A first course in partial differential equations: with complex variables and transform methods*. Courier Corporation, North Chelmsford
- [40] Rwei SP, Huang CC (2012) Electrospinning PVA solution-rheology and morphology analyses. *Fibers Polym* 13:44–50
- [41] Dosunmu OO, Chase GG, Kataphinan W, Reneker DH (2006) Electrospinning of polymer nanofibres from multiple jets on a porous tubular surface. *Nanotechnology* 17:1123
- [42] Dai Y, Sun LL, Ren SL, Ma RD (2013) Finite element optimization of electric field structure in electrospinning. *Adv Mater Res* 765:456–459